Journal of Nuclear Materials 397 (2010) 40–47

Contents lists available at ScienceDirect

Journal of Nuclear Materials

journal homepage: www.elsevier.com/locate/jnucmat

Interpretation and modelling of fission product Ba and Mo releases from fuel

G. Brillant *

Institut de Radioprotection et de Sûreté Nucléaire, DPAM, SEMIC, LETR, BP 3, 13115 Saint-Paul-Lez-Durance, France

ARTICLE INFO

Article history:
Received 21 September 2009
Accepted 5 December 2009

ABSTRACT

The release mechanisms of two fission products (namely barium and molybdenum) in severe accident conditions are studied using the VERCORS experimental observations. Barium is observed to be mostly released under reducing conditions while molybdenum release is most observed under oxidizing conditions. As well, the volatility of some precipitates in fuel is evaluated by thermodynamic equilibrium calculations. The polymeric species $(MoO_3)_n$ are calculated to largely contribute to molybdenum partial pressure and barium volatility is greatly enhanced if the gas atmosphere is reducing. Analytical models of fission product release from fuel are proposed for barium and molybdenum. Finally, these models have been integrated in the ASTEC/ELSA code and validation calculations have been performed on several experimental tests.

1. Introduction

The understanding of fission products (FPs) behaviour (i.e., chemical affinities, redistribution within the fuel and release kinetics in various atmospheres) is essential for the evaluation of possible release to the environment (i.e., the source term) in the case of a severe accident. Over the past decades, many separate effect tests and a few global tests have been performed and major advances have been made in the interpretation and the modelling of the complex phenomena involved in FP release. Among the separate effects experiments, the VERCORS program, funded by IRSN[1] and EDF[2], and conducted by CEA[3], has extended the database of FP release from enriched UO_2 and, to a lesser extent, from MOX fuels at elevated temperatures [1]. A survey has been undertaken by IRSN on the interpretation, the modelling and the validation of models for FP release in severe accident conditions. In the following, the main outcomes concerning barium and molybdenum are discussed.

These two elements are both chemically active FP with high fission yields (Ba ~ 11% and Mo ~ 25%). Barium largely contributes to the residual power of nuclear reactors via its radioactive decay $^{140}Ba \rightarrow {}^{140}La$ (around 20% of the residual power is due to both ^{140}Ba and ^{140}La from 1 to 8 days after a Pressurized Water Reactor (PWR) shutdown). Therefore, the evaluation of the release fraction of barium is necessary to determine the severe accident scenario, especially the possible vessel breakthrough and the resulting start of molten core concrete interaction. In addition, barium and molybdenum have an impact on health, especially on lungs and bones [2]. Beyond its high fission yield and radiological effects, molybdenum can interfere in the release of other FPs since the Mo/MoO_2 couple is known to control the fuel oxygen potential and by chemical interactions (for example form compounds with cesium, strontium, or barium).

The first part of this paper is devoted to the interpretation of barium and molybdenum releases in VERCORS experiments and to some comparisons with other similar studies. In the second part, thermodynamic equilibrium calculations are performed in order to estimate possible chemical mechanisms and major vapour species that are involved in FP release. Then, models of barium and molybdenum releases, dedicated to severe accident simulation tools, are proposed. Lastly, these models of FP release are implemented in the ASTEC/ELSA code [3] and are validated on VERCORS, HCE, and MCE experiments.

2. Interpretation of Ba and Mo releases in VERCORS tests

Due to the potentially severe radiological consequences of a nuclear accident, the VERCORS program [1], which simulates severe PWR accidents, was initiated in order to quantify the emission rates and release kinetics of FP from irradiated nuclear ceramics (enriched UO_2 and MOX fuels) and to consider mitigating measures. Most of the VERCORS tests were conducted with a fuel rod segment composed of three UO_2 irradiated pellets within a zircaloy cladding [1] (see Table 1 for main experimental conditions). Two tests, namely RT3 and RT4, were performed with a rubble-bed geometry (the diameter of the debris ranges from 2 to 4 mm). RT4 was composed of a mixed UO_2/ZrO_2 debris bed and was carried out under oxidizing conditions, while RT3 was composed of a UO_2 debris bed without zirconia and was carried out in an atmosphere of thermodynamic equilibrium with regard to the UO_2.

* Tel.: +33 442 19 94 41; fax: +33 442 19 91 67.
E-mail address: guillaume.brillant@irsn.fr.
[1] Institut de Radioprotection et de Sûreté Nucléaire.
[2] Electricité de France.
[3] Commissariat à l'Energie Atomique.

0022-3115/$ - see front matter © 2009 Elsevier B.V. All rights reserved.
doi:10.1016/j.jnucmat.2009.12.004

Table 1
VERCORS experimental conditions and overall release fractions for Cs, Ba, Mo, Ru, and Ce.

Test		V4	V5	HT1	HT2	HT3	RT1	RT3	RT4
PWR fuel		UO_2 pellets	UO_2 pellets	UO_2 pellets	UO_2 pellets	UO_2 pellets	UO_2 pellets	UO_2 rubble bed	UO_2/ZrO_2 rubble bed
Burnup (GWd/tU)		38.3	38.3	49.4	49.3	47.7	47.3	39.0	37.6
Re-irradiation		yes	yes	yes	yes	yes	no	yes	no
T_{max} (K)		2570	2570	2900	2420	2680	2570	2970	2520
End test	H_2O	–	25	–	25	–	25	1.25	14.6
Atmosphere	H_2	0.2	–	0.2	–	0.2	0.5	1.25	0.4
(mg/s)	He	8	–	8	–	8	–	2	–
Release fraction									
Cs (%)		93	93	100	100	100	100	100	96
Ba (%)		80	55	49	38	85		94	>50
Mo (%)		47	92	49	100	33	70	33	100
Ru (%)		6	6	8	65	6	9	2	8
Ce (%)		3	<3	5	1	1	3	1	3

Samples were re-irradiated just before the test (except the RT1 and RT4 tests) in order to re-create short half-life decay fission products. Then, a temperature transient was applied to these samples under various flowing atmospheres (pure steam, pure hydrogen, air or steam/hydrogen mixture). In each test, a temperature plateau was realised (at around 1500–1700 K), under an oxidizing gas flow, in order to get full oxidation of the cladding. Then, the fuel temperature was increased up to the range [2400; 2900] K depending on the test. During the experiments, FP release kinetics were measured by on-line γ-spectrometry.

In the following, the focus is on UO_2 fuels with medium burnups of about 40–50 GWd/tU. The main VERCORS tests conditions with medium burp-ups fuels are summarized in Table 1 along with the overall release fractions of cesium, barium, molybdenum, ruthenium, and cerium. FPs can be classified depending on their degree of volatility: volatile (FPs that have high releases and are rapidly released; and the release is mainly governed by atomic diffusion within fuel grains), semi-volatile (FPs with potentially large release fractions - the redox conditions can substantially enhance or reduce the release fractions; and the evaporation of chemical compounds is the key-step of the release), low-volatile (FPs that have low releases even at high temperatures and under all redox conditions) and non-volatile (the release of these FP is connected to fuel vaporization). The FPs, with release fractions that are reported in Table 1, are representative of these classes. Thus cesium has a volatile behaviour in VERCORS since it is almost completely released during the tests. Barium and molybdenum can be included among the semi-volatile fission product group with release fractions measured from 33% to 100%. For a given fuel (*e.g.*, comparing V4 and V5), barium is more released under reducing conditions whereas molybdenum is more released under oxidizing conditions. Ruthenium shows very extreme variations [4]. On one hand, ruthenium is a low volatile fission product and it is only slightly released under reducing and low oxidizing conditions (<10%). On the other hand, ruthenium had a high and rapid release under highly oxidizing conditions (65% in HT2 test). Lastly, cerium is a low volatile fission product with final release fractions that do not exceed 5%.

2.1. Barium

Barium is a semi-volatile fission product that is more released under reducing conditions (80% in V4, 85% in HT3) than under oxidizing conditions (55% in V5, 38% in HT2). However, the final release fraction for VERCORS HT1 test (49%) is not as high as expected with a reducing gas atmosphere. This may be due to the slower fuel reducing kinetics in this test since the shape of the crucible used in this test led to limited gas access to the fuel surface in comparison with the other tests. Alternatively, barium release may have been reduced by the early fuel liquefaction observed in this test.

In most tests, barium release starts for temperatures higher than 2000 K and is noticeably slower than for Cs or Mo (see Fig. 1). This is consistent with AECL HCE3 and HCE4 experiments [5,6]. Indeed, no statistically significant releases of barium were measured in HCE4 from bare and clad segments heated to 1920 K under inert or highly oxidizing atmospheres. In HCE3, less than 5% of barium was released from clad samples heated between 1800 K and 2200 K under oxidizing conditions.

In VERCORS RT3 test, in which a UO_2 rubble-bed without zirconium is considered, barium has a specific behaviour. In this test, a small barium release is observed to start early (at about 1750 K, see Fig. 2) and the release kinetics is similar to that of xenon. The same trend has been observed in the global test PHEBUS FPT4 with a rubble-bed geometry, since about 16% of barium was measured in the first filter which corresponds to temperatures lower than 1800 K. This early release of barium from fragments has not been observed in AECL HCE4 experiments with fuel fragments (tests J05, J06, J09, and J10 at 1920 K under (Ar, 2% H_2) atmosphere) [6] or in MCE1 experiments (no Ba release in MCE1-5 test at 2073 K under (Ar, 2% H_2) atmosphere) [7,8]. The interpretation of the low release of barium in AECL tests may be twofold. Firstly, the nature of the atmosphere (no steam in the AECL gas atmosphere in contrast to the VERCORS RT3 atmosphere) can lead to different dominant species of barium (the impact of $BaOH_{(g)}$ and $Ba(OH)_{2(g)}$ on the overall barium partial pressure will be highlighted in the

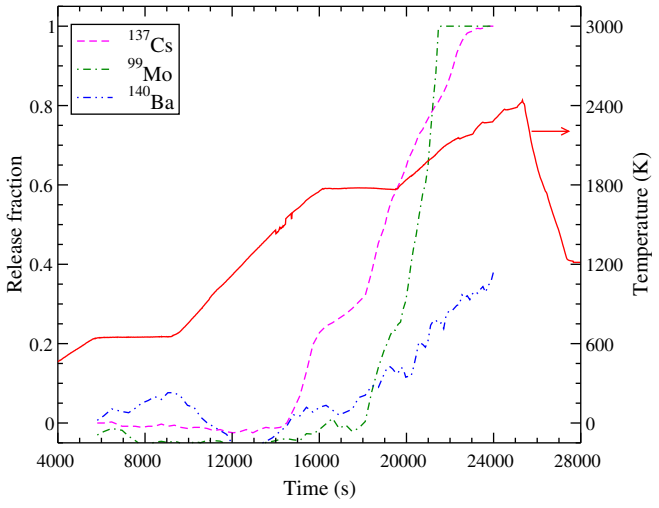

Fig. 1. FP release kinetics in VERCORS HT2 test.

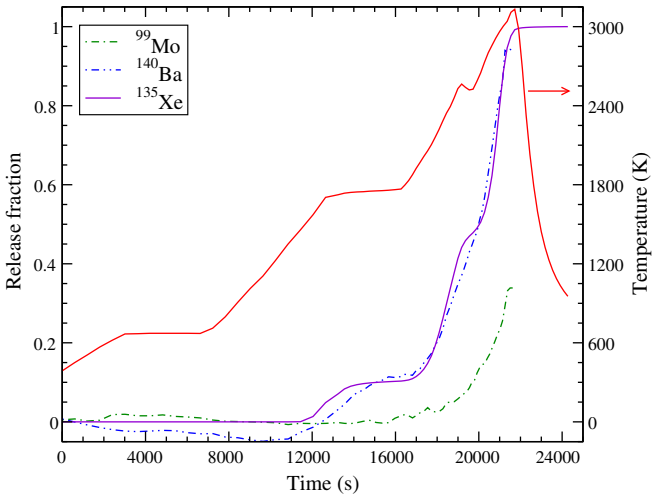

Fig. 2. FP release kinetics in VERCORS RT3 test.

next section). Secondly, the first oxidizing step in VERCORS RT3 test may have modified barium distribution and chemical state within the fuel and, therefore, the next release step. Indeed, barium release has been observed, by Knudsen cell mass spectrometry, to be strongly enhanced by a pre-oxidation treatment of the fuel sample [9,10].

As far as the specific behaviour of barium in RT3 test is concerned, this raises the question to what extent zirconium affects barium release. The VERCORS 5 post-test γ-tomography (see Fig. 3) revealed some barium located in the cladding. Possibly, barium can be trapped by cladding as precipitates that may be barium zirconates (*e.g.*, $BaZrO_3$). As such precipitates can also be formed in the fuel, micro-characterization of some VERCORS samples are planned and will be analyzed in a forthcoming study.

A large fraction of barium was deposited in the vicinity of fuel specimens, as shown in analytical tests carried out by AECL [5]. No barium was detected downstream the impactors of the VERCORS facility. Therefore, barium is probably transported only in aerosol form.

2.2. Molybdenum

Molybdenum is a semi-volatile fission product which is highly released under oxidizing conditions (92% in VERCORS V5 test, 100% in HT2, and 70% in RT1 tests) but shows only half as much release under reducing conditions (47% in VERCORS V4 test, 33% in HT3 test). This impact of redox conditions on molybdenum release has also been observed in other FP release experiments such as HEVA [11], and ORNL experiments of fission product release from horizontal (HI) and vertical (VI) irradiated fuel segments [12,13]. Moreover, molybdenum release has been observed to be more pronounced from pre-oxidized fuel [14].

Molybdenum release fraction is higher in HT1 than in HT3 which can be explained by the less oxidizing conditions in the HT3 test. This is coherent with the lower release of barium in the HT1 test as noted above. In HT2 test, about 20% Mo release was measured at the end of the oxidation plateau at 1770 K (see Fig. 1). Molybdenum was fully released at quite low temperatures (~2100 K). This implies that molybdenum release kinetics becomes faster as the fuel oxygen potential is increasing.

3. Thermodynamic stability of Ba and Mo in fuel

In order to evaluate barium and molybdenum volatility from precipitates, thermodynamic equilibrium calculations are performed using the MEPHISTA database and the GEMINI2 tool which are developed by Thermodata with IRSN support [15]. MEPHISTA database is dedicated to the study of FP behaviour in nuclear fuels.

3.1. Barium

Barium has a low solubility in nuclear fuel [16,17] and has been observed to precipitate as barium oxide BaO [18–20], barium zir-

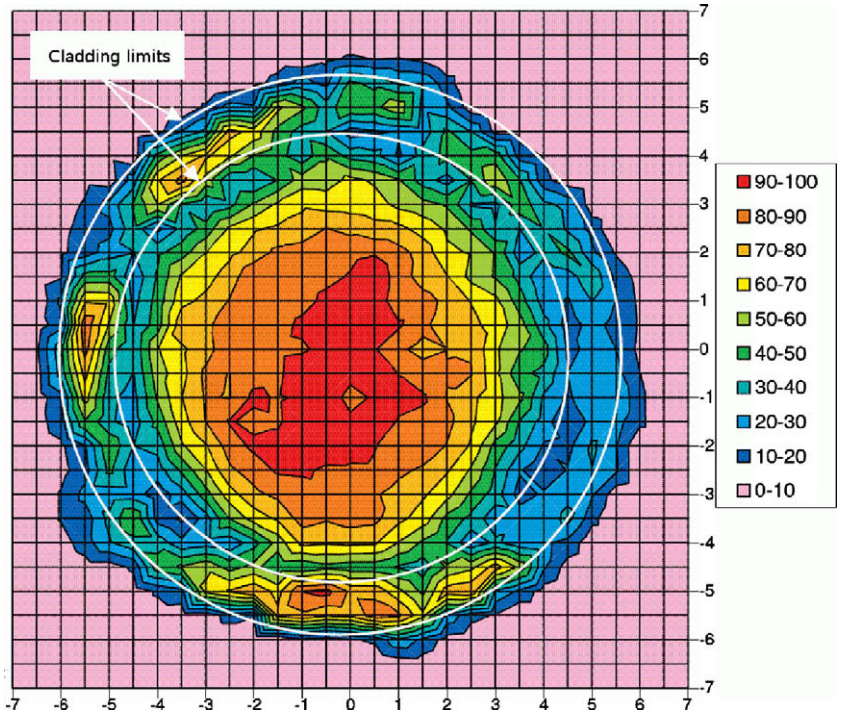

Fig. 3. Barium post-test γ-tomography for VERCORS 5 (arbitrary unit).

conate $BaZrO_3$ [21,20], barium uranate $BaUO_3$ [16,17], and as a complex phase (so called "grey phase") that can be written as (Ba,Sr,Cs) (Zr,U,Pu,Mo,RE)O_3 [16,22–24] and which is mainly $BaZrO_3$. However, no precipitate was observed in a 50 GWd/tM UO_2 fuel [25]. It seems that barium precipitates either in higher burnup fuels or in samples that were exposed to high temperatures.

According to atomic scale calculations, barium solubility in fuel increases with the fuel oxygen potential. By using the density functional theory (DFT) with the Hubbard U correction (which describes the strongly correlated uranium 5f electrons), it has been noticed that BaO is calculated to be soluble in uranium dioxide whatever the stoichiometric regime [26] whereas with empirical potential, BaO is only soluble in hyper-stoichiometric fuel [27]. It has also been shown that barium dissolution in the fuel matrix is energetically preferred to the formation of both ternary phases $BaUO_3$ and $BaZrO_3$ [26].

At first, barium distribution was evaluated using a GEMINI2 calculation with the MEPHISTA database for a barium concentration of 0.4 at.%. For temperatures lower than 1700 K, barium is calculated to be mostly in $BaUO_3$ perovskite structure (see Fig. 4). For higher temperatures, barium is thermodynamically stable in solid solution in the $UO_{2\pm x}$ matrix (fluorite phase) or in the liquid urania phase when present. As far as severe accident scenarios are considered, barium is expected to evolve differently depending on its form. For medium burnup fuels, barium may be mostly dissolved in the matrix at the beginning of the accident, then diffuse to grain boundaries as temperature increases, and can finally be released or take part to the formation of a separate phase. Zirconium diffuses slower than barium in uranium dioxide [20] and is probably not located at grain boundaries in the first part of the accident scenario for a medium burnup PWR UO_2 pellet. Therefore, the separate phases can only be barium oxide or barium uranate as long as zirconium has not reached the boundary of the grain. Later on, as temperature increases, zirconium and barium can react to form barium zirconates. Since there are always some discrepancies between the thermodynamic equilibrium state and experimental observations of irradiated samples, careful interpretation of the results of thermodynamic calculations is required. In the following, the estimation of barium volatility is divided into two parts: barium in the fuel matrix and barium in ternary compounds.

Hereafter, barium in the fuel grains is considered to be either Ba or BaO depending on temperature and the fuel's stoichiometric deviation. Six vapour species are taken into account: Ba, BaO, Ba_2O, BaOH, $Ba(OH)_2$, and BaH. The atmosphere is composed of an H_2, H_2O, and O_2 mixture. One can notice on Fig. 5 that major contributors to barium partial pressure at high temperatures are BaOH and BaO at high oxygen potentials and Ba at low fuel oxygen potentials. An high partial pressure of $Ba(OH)_2$ can also be observed at low temperatures and high oxygen potentials. In all cases, the Ba_2O and BaH contributions to overall barium partial pressure can be neglected. If the atmosphere does not contain hydrogen, the overall barium partial pressure is noticed to be highly reduced (see Fig. 6). For instance, at $T = 2000$ K and $\Delta G_{O_2} = -500$ kJ/mol($p_{O_2} = \exp(\Delta G_{O_2}/RT) = 8.7 \times 10^{-14}$), the overall barium partial pressure is six times lower for a gas atmosphere made of O_2 and Ar than for a gas atmosphere composed of an equilibrium mixture of O_2, H_2, and H_2O ($p_{H_2}/p_{H_2O} \sim 10^3$).

In case of an accident scenario with a rubble bed formation, the atmosphere contains some hydrogen and leach the fuel fragments. In such conditions, barium release may be enhanced by formation of BaOH and $Ba(OH)_2$ species in the gas atmosphere. This could partially explain the early release of barium in VERCORS RT3 and PHEBUS FPT4 experiments.

Barium is also present in the grey phase, which has a perovskite structure. Analyzing this phase can be very complex since many elements are involved, which leads to numerous chemical compounds, some of which can be non-stoichiometric (*e.g.*, $BaUO_{3\pm x}$ or $BaUO_{4\pm x}$). Thermodynamic properties of these compounds have not been fully determined, nor the ternary phase diagrams well understood. Consequently, an extensive study cannot be per-

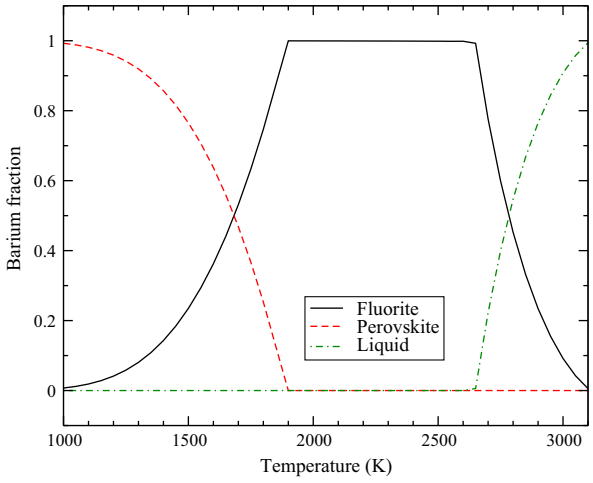

Fig. 4. Distribution of barium between the phases: fluorite (UO_2), perovskite ($BaUO_3$), and liquid UO_2.

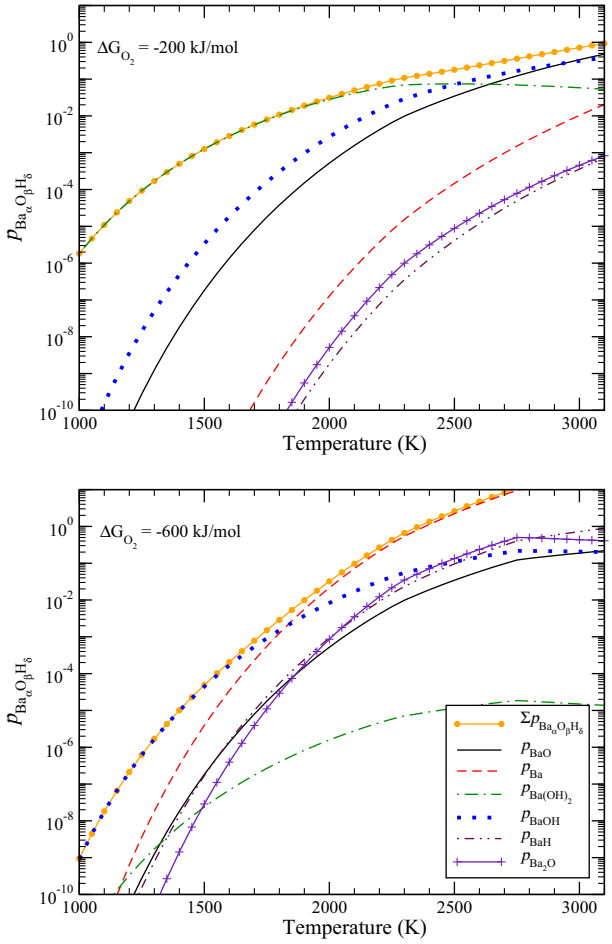

Fig. 5. Barium compound partial pressures calculated over $Ba_{(s)}/BaO_{(s)}$ for $\Delta G_{O_2} = -200$ kJ/mol $\Delta G_{O_2} = RT\ln(p_{O_2})$, then $p_{O_2} \in [3.5 \times 10^{-11}; 6.3 \times 10^{-4}]$ for $T \in [1000; 3000]$ K) and $\Delta G_{O_2} = -600$ kJ/mol($p_{O_2} \in [4.4 \times 10^{-32}; 3.5 \times 10^{-11}]$ for $T \in [1000; 3000]$ K).

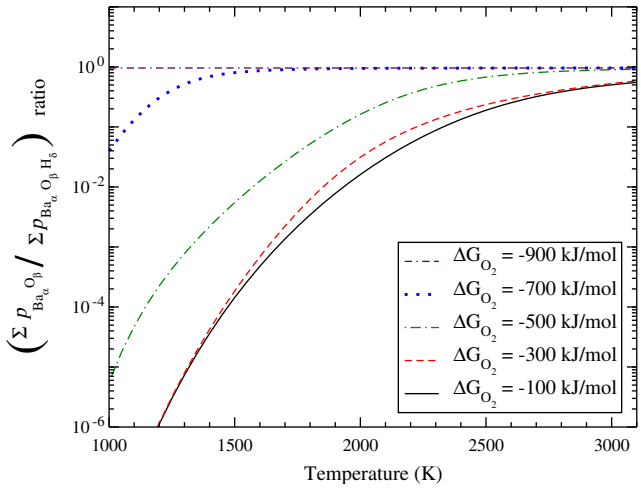

Fig. 6. Impact of hydrogen in gas atmosphere on barium vapour composition. $\Sigma p_{Ba_\alpha O_\beta}$ is calculated considering an atmosphere composed of O_2 and Ar. $\Sigma p_{Ba_\alpha O_\beta H_\delta}$ is calculated considering an equilibrium atmosphere composed of O_2, H_2, and H_2O (*e.g.*, at $\Delta G_{O_2} = -300$ kJ/mol and for $T \in [1000; 3000]$ K, p_{H_2}/p_{H_2O} ratio ranges from 6×10^{-3} up to 21).

formed and the focus shifts to the four main stoichiometric compounds $BaUO_3$, $BaZrO_3$, $BaMoO_3$, and $BaMoO_4$ to evaluate barium partial pressure in accidental conditions. When molybdenum is present, barium partial pressure due to $BaMoO_{4(g)}$ has to be estimated. The partial pressure of $BaMoO_{4(g)}$ over both $BaMoO_{3(s)}$ and $BaMoO_{4(s)}$ is plotted on Fig. 7a and compared to the partial pressure of barium and its oxides ($\Sigma p_{Ba_\alpha O_\beta}$). It was observed that the overall barium partial pressure over $BaMoO_{3(s)}$ and $BaMoO_{4(s)}$ is dominated by $BaMoO_{4(g)}$. Nevertheless, molybdenum has quite a low concentration in the grey phase [24] and may consequently have a low activity coefficient in this phase. Thus, the calculated $BaMoO_{4(g)}$ contribution to the overall barium partial pressure may represent a maximum and can be overestimated by a factor of at least 10. The overall barium partial pressure above BaO, $BaUO_3$, $BaZrO_3$, $BaMoO_3$, and $BaMoO_4$ are gathered on Fig. 7b. One can see that, except for very low oxygen potentials, the barium overall partial pressure is higher over $BaO_{(s)}$ than over the ternary Ba-X-O compounds. To extend these calculations with pure species to in-pile conditions, one has to take care of some possible discrepancies: (i) disturbance from thermodynamic equilibrium state by irradiation; (ii) barium partial pressure over Ba in solid solution in the UO_2 has to be reduced by its activity (estimated as its concentration at a first approximation, i.e., ideal behaviour) and (iii) as discussed above, $BaMoO_{4(g)}$ contribution may also be overestimated. However, the main observation is that the grey phase, as long as it is thermodynamically stable, may capture barium and limit its release.

3.2. Molybdenum

In fuel, molybdenum can exist either in solid solution within the $UO_{2\pm x}$ matrix, in metallic precipitates (the noble metal "white" phase) and, occasionally, in the grey phase [28–31] (at the fuel-cladding gap of certain fuels for example). The solubility of molybdenum in urania was calculated to be very limited using atomic scale calculations [32]. Cesium molybdate (Cs_2MoO_4) is suspected to participate in molybdenum redistribution within the fuel and in molybdenum release from fuel [33,29,31,34]. Since a very low content of Mo is observed in the grey phase, the impact of $BaMoO_{4(g)}$ on molybdenum release is neglected hereafter. Consequently, the volatility of molybdenum is evaluated from either

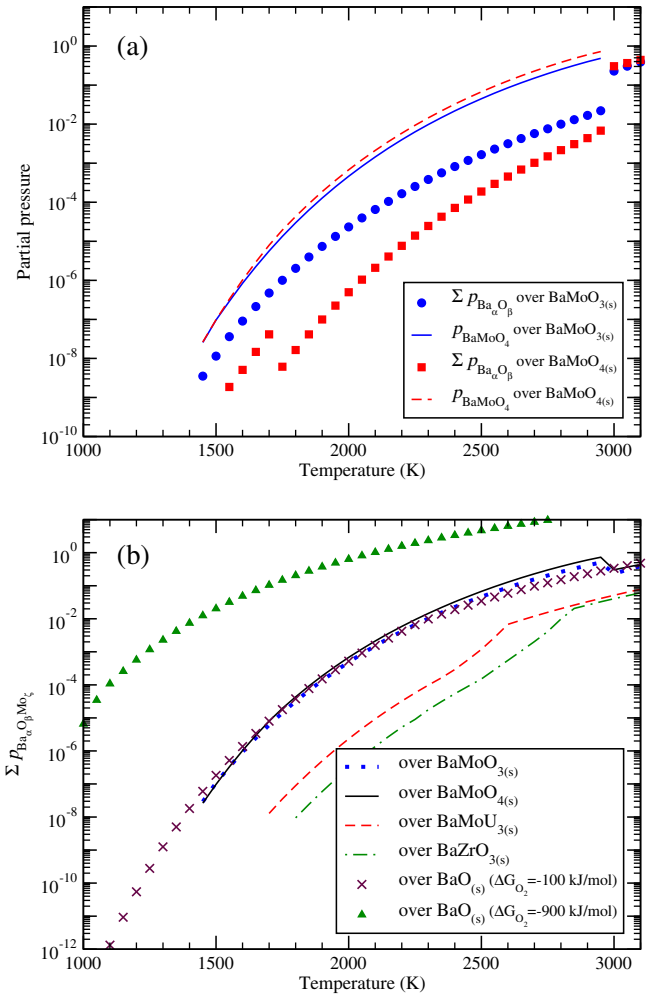

Fig. 7. Variation of partial pressure of barium over some ternary compounds with temperature: (a) partial pressure of barium and its oxides ($\Sigma p_{Ba_\alpha O_\beta}$) and partial pressure of barium molybdate (p_{BaMoO_4}) over $BaMoO_{3(s)}$ and $BaMoO_{4(s)}$ and (b) partial pressure of barium, its oxides and barium molybdate ($\Sigma p_{Ba_\alpha O_\beta Mo_\zeta}$) over various Ba-X-O ternary and BaO binary compounds.

$Mo_{(s)}$ or $MoO_{2(s)}$ and the vapour species $Mo_{(g)}$, $MoO_{(g)}$, $MoO_{2(g)}$, $MoO_{3(g)}$, polymers of $MoO_{3(g)}$, and also $Cs_2MoO_{4(g)}$. Partial pressure of all these species at 2000 K are reported on Fig. 8. It can be observed that $MoO_{3(g)}$ and its polymers contribute to the major part of the total molybdenum compounds partial pressure as the fuel oxygen potential goes above -330 kJ/mol ($p_{O_2} = 2.4 \times 10^{-9}$) at $T = 2000$ K. Gaseous cesium molybdate, that is considered here to be formed from gaseous cesium and solid molybdenum, has also a large impact, even for low cesium partial pressures (see Fig. 9). Cesium molybdate partial pressure is higher at low temperatures but is limited by its saturation vapour pressure at temperatures below 1700–1400 K depending on the cesium partial pressure (as pointed out on Fig. 9).

4. Ba and Mo release modelling

In nuclear safety analyzes, within the severe accident domain, the ASTEC code [3] aims at evaluating the consequences of any accident scenario. Fission products and structural materials releases from the core are evaluated by the ELSA module coupled with the core degradation module DIVA. For solid fuel, FPs are classified into three classes, depending on their degree of volatility (volatile, semi-volatile, and non-volatile). For semi-volatile FPs,

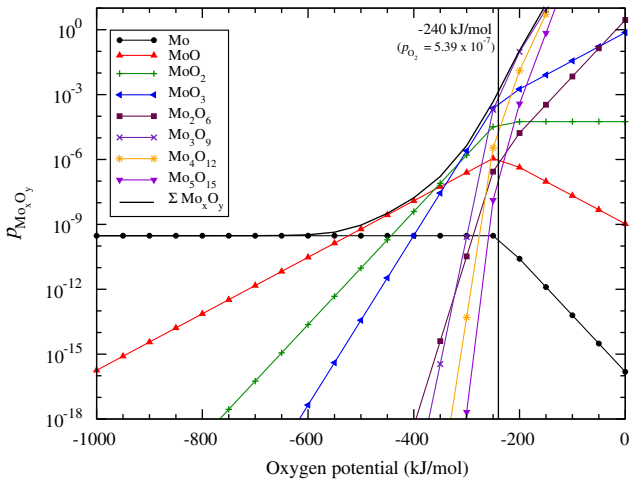

Fig. 8. Molybdenum partial pressure over $Mo_{(s)}$/ $MoO_{2(s)}$ at $T = 2000$ K.

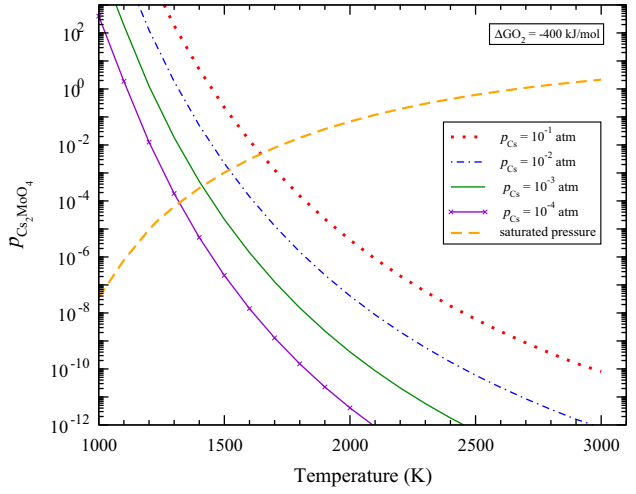

Fig. 9. Impact of cesium partial pressure on cesium molybdate partial pressure at $\Delta G_{O_2} = -400$ kJ/mol and for $T \in [1000; 3000]$ K(*i.e.*, $p_{O_2} \in [1.27 \times 10^{-21}; 1.08 \times 10^{-7}]$).

such as Ba and Mo, the release from the open fuel porosities is assumed to be governed by evaporation and mass transfer processes. Therefore, correlations of the overall FP partial pressures are required by ASTEC/ELSA to calculate the release rate of semi-volatile FPs. In the following, analytical models are proposed for barium and molybdenum and are validated on some VERCORS, HCE, and MCE experiments.

4.1. Models description

Barium release modelling takes into account the volatilization of barium in solid solution of the form $Ba_{(s)}$ or $BaO_{(s)}$, using chemical reactions b, c, d, e, f, depending on the fuel oxygen potential. The equilibrium potential $\Delta G^{limit}_{Ba/BaO}$ between $Ba_{(s)}$ and $BaO_{(s)}$ is estimated with Eq. (1) and corresponds to the reaction (a). The equilibrium constants $K_{[b]}$ to $K_{[f]}$ for reactions b, c, d, e, f are calculated using Table 2. Hereafter, all the given correlations for equilibrium constants or potentials were obtained by best fit estimations of the data from the MEPHISTA database.

$$BaO_{(c)} = Ba_{(c)} + 0.5O_{2(g)} \quad (a)$$
$$BaO_{(c)} = BaO_{(g)} \quad (b)$$
$$Ba_{(c)} = Ba_{(g)} \quad (c)$$

Table 2
Data for the evaluation of equilibrium constants for barium volatilization obtained by best fit estimations of the data from the MEPHISTA database ($R = 8.314$ J/(mol K)).

$K_{[.]} = \exp\{-(A + BT + CT^2)/(RT)\}$			
Reaction	A (J/mol)	B (J/(mol K))	C (J/mol K^{-2})
(b)	4.52×10^5	−206	2.13×10^{-2}
(c)	1.71×10^5	−81.2	–
(d)	3.35×10^5	−49.0	–
(e)	-2.35×10^5	82.9	–
(f)	-1.36×10^5	44.6	–

$$BaO_{(g)} = Ba_{(g)} + 0.5O_{2(g)} \quad (d)$$
$$BaO_{(g)} + H_2O_{(g)} = Ba(OH)_{2(g)} \quad (e)$$
$$BaO_{(g)} + 0.5H_{2(g)} = BaOH_{(g)} \quad (f)$$

$$\Delta G^{limit}_{Ba/BaO} = -1.08 \times 10^6 + 122T + 6.85 \times 10^{-2} T^2 - 1.64 \times 10^{-5} T^3 \quad (1)$$

Considering that the most important solid form of barium is Ba for low oxygen potential (actually $\Delta G_{O_2} < \Delta G^{limit}_{Ba/BaO}$) and BaO otherwise, the volatility of barium is evaluated with its overall partial pressure (p^{tot}_{Ba}) which is the sum of the partial pressures of the gaseous forms of barium and its oxides. Then, the model for barium release is based on correlations (1)–(3) and consists of the following expression:

- if $\Delta G_{O_2} < \Delta G^{limit}_{Ba/BaO}$

$$p^{tot}_{Ba} = X_{Ba} K_{[c]} \left\{ 1 + \frac{(p_{O_2})^{0.5}}{K_{[d]}} \times \left[1 + K_{[e]} \cdot p_{H_2O} + K_{[f]} \cdot (p_{H_2})^{0.5} \right] \right\} \quad (2)$$

- otherwise

$$p^{tot}_{Ba} = X_{Ba} . K_{[b]} \left[1 + K_{[d]} \cdot (p_{O_2})^{-0.5} + K_{[e]} . p_{H_2O} + K_{[f]} \cdot (p_{H_2})^{0.5} \right] \quad (3)$$

where X_{Ba} denotes the barium concentration in fuel. Note that for clad samples, hydrogen and steam are not supposed to be in contact with fuel and, hence, $K_{[e]}$ and $K_{[f]}$ can be ignored when intact clad geometries are considered.

The proposed modelling of molybdenum release is based on the volatility of molybdenum in solid solution either in the metallic or in the oxide phases depending on the fuel's stoichiometric deviation. The equilibrium potential between these two phases is evaluated using the following correlation which was set up using data from the MEPHISTA database:

$$\Delta G^{limit}_{Mo/MoO_2} = -5.88 \times 10^5 + 192T - 9.05 \times 10^{-3} T^2 \quad (4)$$

Release from the metallic phase is estimated through chemical reactions (g) and (h) and Eqs. (5) and (6). The release from the oxide phase is evaluated thanks to chemical reactions (i) and (j) and Eqs. (7) and (8). The calculated partial pressure for cesium molybdate is limited to its saturated partial pressure (reaction (k) and (9)).

$$\alpha Mo_{(s)} + \beta O_{2(g)} = Mo_\alpha O_{2\beta(g)} \quad (g)$$
$$Mo_{(s)} + 2Cs_{(g)} + 2O_{2(g)} = Cs_2MoO_{4(g)} \quad (h)$$
$$\alpha MoO_{2(s)} + (\beta - \alpha)O_{2(g)} = Mo_\alpha O_{2\beta(g)} \quad (i)$$
$$MoO_{2(s)} + 2Cs_{(g)} + O_{2(g)} = Cs_2MoO_{4(g)} \quad (j)$$
$$Cs_2MoO_{4(c)} = Cs_2MoO_{4(g)} \quad (k)$$

$$K^{-}_{\alpha\beta} = \frac{p_{Mo_\alpha O_{2\beta}}}{(p_{O_2})^{\beta}} \quad (5)$$

$$K_1 = \frac{p_{Cs_2MoO_4}}{(p_{Cs})^2 (p_{O_2})^2} \quad (6)$$

$$K^{+}_{\alpha\beta} = \frac{p_{Mo_\alpha O_{2\beta}}}{(p_{O_2})^{\beta-\alpha}} \quad (7)$$

$$K_2 = \frac{p_{Cs_2MoO_4}}{(p_{Cs})^2 p_{O_2}} \quad (8)$$

$$p^{sat}_{Cs_2MoO_4} = \exp\left(-15.6 + \frac{3.52 \times 10^4}{T}\right) \quad (9)$$

Therefore, the overall molybdenum partial pressure (p^{tot}_{Mo}), which is the sum of the partial pressures of all the gaseous forms of molybdenum, can be calculated using correlations (4)–(11) as follows (considering that the most important solid form of molybdenum is Mo for low oxygen potential (actually $\Delta G_{O_2} < \Delta G^{limit}_{Mo/MoO_2}$) and MoO_2 otherwise):

- if $\Delta G_{O_2} < \Delta G^{limit}_{Mo/MoO_2}$

$$p^{tot}_{Mo} = X_{Mo}\left[\Sigma_{\alpha,\beta}\left(K^{-}_{\alpha\beta} \cdot p^{\beta}_{O_2}\right) + \min\left(K_1 (p_{Cs})^2 (p_{O_2})^2, p^{sat}_{Cs_2MoO_4}\right)\right] \quad (10)$$

- otherwise

$$p^{tot}_{Mo} = X_{Mo}\left[\Sigma_{\alpha,\beta}\left(K^{+}_{\alpha\beta} \cdot p^{\beta-\alpha}_{O_2}\right) + \min\left(K_2 (p_{Cs})^2 p_{O_2}, p^{sat}_{Cs_2MoO_4}\right)\right] \quad (11)$$

where X_{Mo} is the molybdenum concentration in fuel, $p^{sat}_{Cs_2MoO_4}$ is evaluated thanks to Eq. (9) and the $K^{-/+}_{\alpha\beta}$ are calculated using Table 3.

4.2. Validation of the models

These two models have been implemented in the ASTEC/ELSA code and subsequently used for the calculations of VERCORS, HCE and MCE experiments. Calculated release kinetics of barium and molybdenum agree quite well with experimental measurements for both oxidizing and reducing atmospheres. For instance, release kinetics are plotted on Fig. 10 for VERCORS V4, with reducing conditions after the oxidation plateau, and for VERCORS V5, with an oxidizing atmosphere during the whole test. Barium release kinetics is very well reproduced by the calculation for the two tests even if the final release fraction is slightly overestimated in V5 test (60% calc. and 55% exp.) and underestimated in V4 test (72% calc. and 80% exp.). The calculated release kinetics of molybdenum is 1400 s too late for VERCORS V5 test, possibly owing to a slight underestimation of the fuel oxidation kinetics (although the total calculated release fraction matches the experimental value very well). However, there are discrepancies between calculated and measured Mo release kinetics in VERCORS V4 in both the rate (kinetics) and in the final release (25% calc. and 45% exp.). There is also a slight Mo release during the oxidation plateau but this is hardly seen in the calculation. This may be partially due to some inaccuracies in the calculation of the fuel oxidation kinetics by ASTEC that impact the estimation of the semi-volatile FPs partial pressure and their release kinetics.

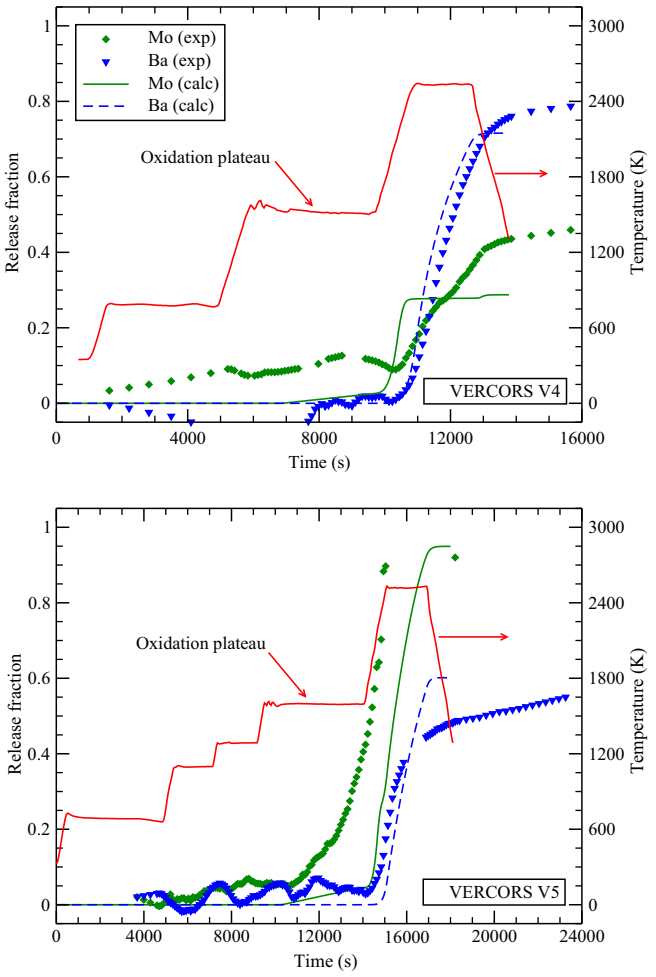

Fig. 10. Comparison of experiments and calculations for molybdenum and barium release kinetics in VERCORS V4 and V5 tests.

The simulation of the highly reducing test VERCORS HT1 led to the largest discrepancies between experiment (49% for Mo, 49% for Ba) and calculations (17% for Mo, 89% for Ba). For the other tests, the differences between experiment and simulation are rather low and the comparison of the overall fractional release leads to overall satisfactory results, even if some discrepancies remain in some tests (see Table 4). Furthermore, the impact of the redox regime of the atmosphere on the fractional release is well reproduced by ASTEC calculations. Further, the barium and molybdenum release modelling seems to be applicable to both clad and rubble-bed geometries. The high release fractions of Ba estimated for both RT3 and RT4 tests matches the experimental data.

Barium release modelling was also validated on the basis of AECL tests with clad samples: the HCE3 series [5], and with fragments (small pieces of fuel): the MCE1 series [8]. With these tests, the validation database has been extended to include air ingress scenario and inert atmospheres. Though some differences between measurements and calculations can be noticed on Table 5, the major trends are reproduced by calculations and permit the validation

Table 3
Data for the evaluation of equilibrium constants for molybdenum volatilization $K^{-/+}_{\alpha\beta} = \exp(A_0 + A_1/T)$ obtained by best fit estimations of the data from the MEPHISTA database.

Species	$K^{-}_{\alpha\beta}$		$K^{+}_{\alpha\beta}$	
	A_0	A_1 (K)	A_0	A_1 (K)
$Mo_{(g)}$	17.5	-7.88×10^4	37.85	-1.49×10^5
$MoO_{(g)}$	12.3	-3.70×10^4	32.7	-1.07×10^5
$MoO_{2(g)}$	3.93	1.54×10^3	24.3	-6.82×10^4
$MoO_{3(g)}$	−6.78	4.19×10^4	13.6	-2.79×10^4
$Mo_2O_{6(g)}$	−29.0	1.17×10^5	12.8	-2.27×10^5
$Mo_3O_{9(g)}$	−53.6	2.24×10^5	9.20	1.41×10^4
$Mo_4O_{12(g)}$	−76.6	3.07×10^5	7.13	2.64×10^4
$Mo_5O_{15(g)}$	−101	3.88×10^5	3.88	3.80×10^4

Table 4
Global fractional releases in VERCORS tests from experiments and ASTEC/ELSA calculations.

Test	Mo		Ba	
	Exp.	Calc.	Exp.	Calc.
VERCORS V4	47	29	80	72
VERCORS V5	92	95	55	60
VERCORS HT1	49	17	49	89
VERCORS HT2	100	100	39	40
VERCORS HT3	33	47	85	85
VERCORS RT1	>70	85	–	67
VERCORS RT3	33	20	94	100
VERCORS RT4	100	83	>50	84

Table 5
Barium overall fractional releases in AECL HCE3 and MCE1 tests from experiments and ASTEC/ELSA calculations.

Test #	T_{max} (K)	Atmosphere	Release fraction (%)	
			Exp.	Calc.
MCE1				
1	1973	Air	0	10
2	2073	Air	10	22
3	2173	Air	15	48
4	2273	Air	60	68
5	2073	Ar/2% H_2	0	30
6	2273	Ar/2% H_2	40	79
7	2350	Air	90	90
8	2350	Ar/2% H_2 + 100 Pa O_2	95	85
HCE3				
H01	2200	90% H_2O 10% Ar 0.2% H_2	5	16
H02	2160	Air	4	16
H03	2110	87% H_2O 13% Ar 0.3% H_2	2	10
H04	2100	3.5% H_2O 96% Ar 0.5% H_2	2	9
H05	1780	Air	0	0
H06	1810	86% H_2O 13% Ar 0.6% H_2	0	1

of the barium release model. One can observe a general overestimation of barium release under all conditions, excepting oxidizing conditions at the highest temperatures (MCE1 7 and 8 at 2350 K). Reducing conditions show the largest overestimations. Indeed, 30% and 79% of Ba is calculated to be released in MCE1 5 and 6 tests while 0% and 40% were measured experimentally. For the HCE3 tests with cladded samples, the calculated release fractions of Ba are quite low as experimentally observed.

5. Conclusions

Barium and molybdenum releases during VERCORS tests have been discussed. An interpretation of their semi-volatile behaviour is proposed, suggesting their release kinetics are highly influenced by the redox properties of the surrounding atmosphere.

Thermodynamic equilibrium calculations of Ba and Mo volatilization over pure compounds have been carried out. Two FP release models have been developed and have been implemented in ASTEC/ELSA code. Then, these models have been subsequently validated on VERCORS, HCE and MCE test series.

The ability of this mainly thermodynamic approach of FP release from fuel has been demonstrated over a large domain of conditions. In a forthcoming study, this survey of interpretation, modelling, and validation of FP release from fuel will be extended to other semi-volatile FP of high interest for safety studies.

Acknowledgements

B. Clément and D. Vola (IRSN) are gratefully acknowledged for fruitful discussions and advises. The financial support from EdF and the discussions with the CEA team on VERCORS measurements are thanked.

References

[1] G. Ducros, P.P. Malgouyres, M. Kissane, D. Boulaud, M. Durin, Nucl. Eng. Des. 208 (2001) 191.
[2] D.J. Alpert, D.I. Chanin, L.T. Ritchie, Relative importance of individual elements to reactor accident consequences assuming equal release fractions, Tech. rep. NUREG/CR-4467, SAND85-2575, Sandia National Laboratories, Albuquerque, 1988.
[3] J.P. van Dorsselaere, C. Seropian, P. Chatelard, F. Jacq, J. Fleurot, P. Giordano, N. Reinke, B. Schwinges, H. Allelein, W. Luther, Nucl. Technol. 165 (3) (2009) 293.
[4] A. Auvinen, G. Brillant, N. Davidovich, R. Dickson, G. Ducros, Y. Dutheillet, P. Giordano, M. Kunstar, T. Karkela, M. Mladin, Y. Pontillon, C. Seropian, N. Ver, Nucl. Eng. Des. 238 (12) (2008) 3418.
[5] R.D. Barrand, R.S. Dickson, R.S. Liu, D.D. Semeniuk, Release of fission products from CANDU fuel in air, steam and argon atmospheres at 1500–1900 °C: the HCE3 experiment, in: 6th International CNS CANDU Fuel Conference, CNS, Niagara Falls, 1999, pp. 1–10.
[6] L.W. Dickson, R.S. Dickson, Z. Liu, R.D. Barrand, D.D. Semeniuk, Fission-product releases from CANDU fuel heated to 1650 °C: HCE4 experiment, in: 7th International Conference on CANDU Fuel, vol. 2, Kingston, Ontario, Canada, 2001, pp. 3B/21–30.
[7] D. Cox, C.E.L. Hunt, Z. Liu, F.C. Iglesias, N.A. Keller, R.D. Barrand, R.F. O'Connor, A model for the release of low volatility fission products in oxidizing conditions, in: 12th Annual Conference, AECL-10440, CNS, Saskatoon, 1991, pp. 280–289.
[8] D.S. Cox, C.E.L. Hunt, Z. Liu, N.A. Keller, R.D. Barrand, R.F. O'Connor, F.C. Iglesias, Fission product releases from UO_2 in air and inert conditions at 1700–2350 K: analysis of the MCE-1 experiment, in: Safety of Thermal Reactors, AECL-10438, Int. Topical Meeting, ANS, Portland, 1991, pp. 1–20.
[9] J.Y. Colle, J.-P. Hiernaut, D. Papaioannou, C. Ronchi, A. Sasahara, J. Nucl. Mater. 348 (2006) 229.
[10] J.-P. Hiernaut, T. Wiss, D. Papaioannou, R.J.M. Konings, V.V. Rondinella, J. Nucl. Mater. 372 (2008) 215.
[11] J.P. Leveque, B. Andre, G. Ducros, G. Le Marois, G. Lhiaubet, Nucl. Technol. 108 (1) (1994) 33.
[12] M.F. Osborne, J.L. Collins, R.A. Lorenz, Nucl. Technol. 78 (1987) 157.
[13] M.F. Osborne, R.A. Lorenz, Nucl. Safety 33 (3) (1992) 344.
[14] M.A. Mansouri, D.R. Olander, J. Nucl. Mater. 254 (1998) 22.
[15] M. Barrachin, P.Y. Chevalier, B. Cheynet, E. Fischer, A thermodynamic database for nuclear applications, in: MMSNF-5 Workshop, Nice, France, 2006.
[16] C. Sari, C.T. Walker, G. Schumacher, J. Nucl. Mater. 79 (1979) 255.
[17] H. Kleykamp, J. Nucl. Mater. 206 (1993) 82.
[18] C.T. Walker, C. Bagger, M. Mogensen, J. Nucl. Mater. 173 (1990) 14.
[19] W.H. Hocking, A. Duclos, L.H. Johnson, J. Nucl. Mater. 209 (1994) 1.
[20] I. Sato, H. Furuya, T. Arima, K. Idemitsu, K. Yamamoto, J. Nucl. Sci. Technol. 36 (9) (1999) 775.
[21] I.L.F. Ray, H. Thiele, Hj. Matzke, J. Nucl. Mater. 188 (1992) 90.
[22] H. Kleykamp, J.O. Paschoal, R. Pejsa, F. Thümmler, J. Nucl. Mater. 130 (1985) 426.
[23] H. Kleykamp, J. Nucl. Mater. 131 (1985) 221.
[24] P.G. Lucuta, R.A. Verrall, Hj. Matzke, B.J. Palmer, J. Nucl. Mater. 178 (1991) 48.
[25] L.E. Thomas, C.E. Beyer, L.A. Charlot, J. Nucl. Mater. 188 (1992) 80.
[26] G. Brillant, A. Pasturel, Phys. Rev. B 77 (2008) 184110.
[27] R.W. Grimes, C.R.A. Catlow, Philos. Trans. Royal Soc. Lond. A 335 (1991) 609.
[28] M. Tourasse, M. Boidron, B. Pasquet, J. Nucl. Mater. 188 (1992) 49.
[29] I. Sato, H. Furuya, T. Arima, K. Idemitsu, K. Yamamoto, J. Nucl. Mater. 273 (1999) 239.
[30] P. Martin, M. Ripert, G. Carlot, P. Parent, C. Laffon, J. Nucl. Mater. 326 (2004) 132.
[31] K. Maeda, K. Tanaka, T. Asaga, A. Furuya, J. Nucl. Mater. 344 (2005) 274.
[32] G. Brillant, F. Gupta, A. Pasturel, J. Phys.: Condens. Matter 21 (2009) 285602.
[33] I. Sato, H. Furuya, K. Idemitsu, T. Arima, K. Yamamoto, M. Kajitani, J. Nucl. Mater. 247 (1997) 46–49.
[34] J. McFarlane, J.C. Leblanc, D.G. Owen, High-temperature chemistry of molybdenum cesium, iodine and UO_{2+x}, Tech. rep. 11708, AECL, 1996.